2018 IEEE EMBS International Conference on Biomedical & Health Informatics (BHI)
4-7 March 2018
Las Vegas, Nevada, USA

Inverse ECG Modeling with Spatiotemporal Regularization for the Characterization of Myocardial Infarctions

Bing Yao, Rui Zhu, and Hui Yang, *Member, IEEE*

***Abstract*— Myocardial infarctions (MIs) pose a significant risk to human health. Accurate identification and characterization of MI's are essential for the effective medical treatment. Traditional methods such as the standard 12-lead ECG identify MIs with the electrocardiogram (ECG) recorded on the body surface, which consider little about anatomical details of the human body. These methods are limited in the ability to map back the actual electrical activities of the heart and further characterize MIs. Inverse ECG (iECG) methods were proposed to trace the distribution of electric potentials on the heart surface and characterize MIs. However, these methods do not account for the spatiotemporal behaviors of the potential distributions, because the electric potentials are distributed in the complex geometry and varying dynamically over time. In this paper, a novel iECG model with spatiotemporal regularization is developed to image and characterize MIs. We solve the iECG problem with the method of spatiotemporal regularization and reconstruct electric potentials on the heart surface. Furthermore, we group the estimated heart potentials into healthy and infarct clusters with a wavelet-clustering method. Experimental results show that the proposed method effectively solves the iECG problem and better characterizes MIs compared with existing methods.**

I. Introduction

Myocardial infarction (MI), known as heart attack, poses a significant risk to human health. Precise identification and characterization of MIs are urgently needed to conduct the effective medical treatment for MIs and improve life quality. Traditional methods such as the standard 12-lead ECG method, usually record the electrocardiogram (ECG) on the body surface and directly analyze the ECG signal to identify heart abnormalities. In these methods, the obtained information about cardiac electrical activities is limited and with low resolution. Additional leads are added later in the body surface potential mapping (BSPM) to fix this limitation. BSPM is with higher resolution than the standard 12-lead ECG and provides a comprehensive imaging of the dynamic electrical activity on the heart surface for the decision-making of cardiac diseases. However, BSPM accounts little for anatomical details of the human body and is limited in the ability to map back the actual electrical activities of the heart and further characterize the MIs.

Cardiac electrical activity is closely associated with heart electric potentials. Inverse ECG (iECG) methods are developed to identify and characterize MIs, which images the heart potential distribution from body potential distribution [1]. The electric potentials vary dynamically over time and are distributed on the complex human-geometry. However, very little has been done to cope with the spatiotemporal behaviors of electric potentials. This limitation leads to a high relative error between the estimated and true potential distributions on the heart surface. Thus the implementation of iECG models in the pathological decision-making is delayed.

In this paper, a spatiotemporal inverse model is proposed to reconstruct the potential distribution on the heart surface and characterize the location and extent of MIs. First, a transfer matrix is developed to model the relationship between potential distributions on the body and heart surfaces. This transfer matrix is derived from the integration of physics-based principles with the boundary element method. Second, we solve the iECG problem and estimate the heart potential distribution with a novel spatiotemporal regularization method. Finally, the estimated heart potentials are grouped into healthy and infarct clusters with a wavelet-clustering method, and are further used to characterize the location and extent of MIs. Experimental results demonstrate that an effective solution to the iECG problem and better performance in the characterization of MI are achieved by the proposed model compared with existing iECG methods.

This paper is organized as follows: Section II presents the research methodology. Section III describes the experimental design and results. Section IV concludes this paper.

II. Research Methodology

In order to build an effective inverse ECG model, there are several challenges remained to be addressed. First, the complex geometry of the human body makes it difficult to establish a clear relationship between the heart potentials ϕ_H and body potentials ϕ_B and further calculate the transfer matrix $\boldsymbol{R}_{BH}$. Second, ϕ_H and ϕ_B are with high-dimensionality and $\boldsymbol{R}_{BH}$ is rank deficient (i.e., $rank(\boldsymbol{R}_{BH}) < \min\{dim(\phi_H, \phi_B)\}$), which results in an ill-conditioned ECG problem. Third, ϕ_H and ϕ_B are dynamically distributed in the complex torso-heart geometry. In order to address the approximation errors in $\boldsymbol{R}_{BH}$ and improve the model robustness to measurement noise, both the temporal and spatial correlations should be accounted for in the inverse model.

As shown in Fig. 1, we propose a novel spatiotemporal inverse ECG (ST-iECG) model to characterize MIs, whose

This work is supported in part by the National Science Foundation (CMMI-1617148, CMMI-1619648, and IOS-1146882).

Bing Yao, Rui Zhu, and Hui Yang* are with the Complex System Monitoring, Modeling and Analysis Laboratory, The Pennsylvania State University, University Park, PA 16802 USA (*corresponding author: huy25@psu.edu)

978-1-5386-2405-0/18/$31.00 ©2018 IEEE

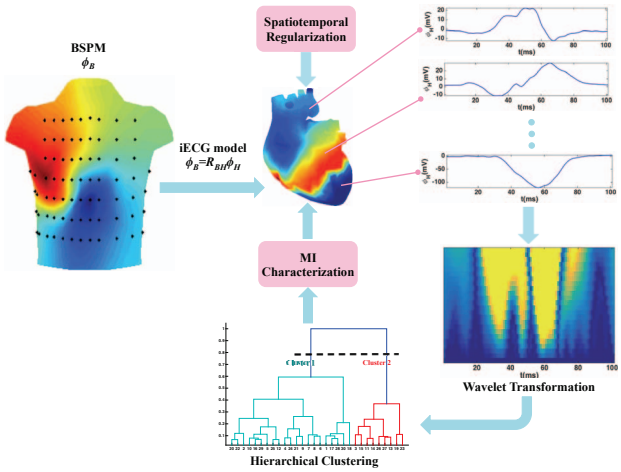

Fig. 1. Flowchart of research methodology.

objective function is formulated as

$$\min_{\phi_H(t)} J = \sum_{t=1}^{T}\{\|\phi_B(t) - \boldsymbol{R}_{BH}\phi_H(t)\|^2 + \lambda_s^2\|\Delta_s\phi_H(t)\|^2 + \lambda_t^2 \sum_{\tau=t-\frac{w}{2}}^{t+\frac{w}{2}} \|\phi_H(t) - \phi_H(\tau)\|^2\} \quad (1)$$

First, we propose to solve the transfer matrix $\boldsymbol{R}_{BH}$ using the boundary element method (BEM) [2] integrated with divergence theorem and Green's second identity. Second, we solve the iECG problem and estimate the heart potential distribution using a new spatiotemporal regularization model [3]. Third, the estimated electrical potentials from step two are grouped into infarct and healthy clusters by a multi-resolution wavelet-clustering method.

A. Derivation of Transfer Matrix $\boldsymbol{R}_{BH}$

The human torso is modeled as a volume conductor [4] bounded by body surface S_B and heart surface S_H, and the heart works as a bioelectric source. In the present investigation, BEM is utilized to derive $\boldsymbol{R}_{BH}$ integrated with divergence theorem and Green's second identity. In this method, S_B and S_H are discretized into triangle meshes. Then, an approximate solution to the integrals derived from the Laplacian equation is obtained. This results in the transfer matrix $\boldsymbol{R}_{BH}$ expressed as $\boldsymbol{R}_{BH} = (\boldsymbol{M}_{BH}\boldsymbol{M}_{HH}^{-1}\boldsymbol{A}_{HH} - \boldsymbol{A}_{BH})^{-1} \times (\boldsymbol{A}_{BB} - \boldsymbol{M}_{BH}\boldsymbol{M}_{HH}^{-1}\boldsymbol{A}_{HB})$, where the coefficient matrices $\boldsymbol{M}$'s and $\boldsymbol{A}$'s are dependent entirely on the geometry of human body [4].

However, $\boldsymbol{R}_{BH}$ is rank-deficient and with a large condition number [1]. The resulted iECG problem is ill-conditioned, i.e., a small measurement noise will result in a big difference in the final solution of the ECG model. Thus, achieving a stable solution of $\boldsymbol{\phi}_H$ call for the integration of these physics-based models with new statistical regularization methods.

B. Spatiotemporal Regularization

The spatial regularity $\lambda_s^2\|\Delta_s\phi_H(t)\|^2$ and the temporal regularity $\lambda_t^2 \sum_{\tau=t-\frac{w}{2}}^{t+\frac{w}{2}} \|\phi_H(t) - \phi_H(\tau)\|^2$ are added in the ST-iECG model to take both spatial and temporal correlations into account [3]. λ_s and λ_t are the spatial and temporal regularization parameters determined by the L-curve method [5]. Matrix Δ_s is the spatial Laplacian on irregular triangle meshes and parameter w denotes a time window.

We propose to estimate ϕ_H using the dipole multiplicative update (DMU) method [3], for the reason that it is difficult to solve for ϕ_H analytically while both the spatial and temporal correlations are involved. DMU method splits the electric potential $\boldsymbol{\phi}_H$ into its positive part $\boldsymbol{\phi}^+$ and negative part $\boldsymbol{\phi}^-$, where $\boldsymbol{\phi}^+$ and $\boldsymbol{\phi}^-$ are defined as $\boldsymbol{\phi}^+ = \max\{0, \boldsymbol{\phi}_H\}$ and $\boldsymbol{\phi}^- = \max\{0, -\boldsymbol{\phi}_H\}$. Thus, we can write $\boldsymbol{\phi}_H$ as $\boldsymbol{\phi}_H = \boldsymbol{\phi}^+ - \boldsymbol{\phi}^-$, and obtain the updating rules for $\boldsymbol{\phi}^+$ and $\boldsymbol{\phi}^-$ in the algorithm shown in Table I.

TABLE I
THE PROPOSED DIPOLE MULTIPLICATIVE UPDATE ALGORITHM

1: Set constants λ_s, λ_t and w .
2: Initialize $\{\boldsymbol{\phi}^+\}$ and $\{\boldsymbol{\phi}^-\}$ as positive random matrices.
3: **Repeat**
4: **for** $t = 1, \ldots, T$ **do**

$$(\boldsymbol{\phi}_t^+)_i \leftarrow \frac{(\boldsymbol{A}\boldsymbol{\phi}_t^-)_i + B_i + \sqrt{((\boldsymbol{A}\boldsymbol{\phi}_t^-)_i + B_i)^2 + 4(\boldsymbol{A}^+\boldsymbol{\phi}_t^+)_i(\boldsymbol{A}^-\boldsymbol{\phi}_t^+)_i}}{(2\boldsymbol{A}^+\boldsymbol{\phi}_t^+)_i}(\boldsymbol{\phi}_t^+)_i$$

$$(\boldsymbol{\phi}_t^-)_i \leftarrow \frac{(\boldsymbol{A}\boldsymbol{\phi}_t^+)_i - B_i + \sqrt{((\boldsymbol{A}\boldsymbol{\phi}_t^+)_i - B_i)^2 + 4(\boldsymbol{A}^+\boldsymbol{\phi}_t^-)_i(\boldsymbol{A}^-\boldsymbol{\phi}_t^-)_i}}{(2\boldsymbol{A}^+\boldsymbol{\phi}_t^-)_i}(\boldsymbol{\phi}_t^-)_i$$

5: **end for**
6: **until convergence**

C. Wavelet Clustering of ECG Time Series

The heart electric potentials $\boldsymbol{\phi}_H$ are dynamically varying and denoted as $\{\phi_H(t)\}_{t=1}^T$. We propose a clustering method with multi-resolution wavelet to analyze $\boldsymbol{\phi}_H$ and avoid the high dimensionality, high correlation and unavoidable uncertainties of the ECG time series, and further group $\boldsymbol{\phi}_H$ into healthy and infarct clusters.

In the wavelet transformation, $\boldsymbol{\phi}_H$ is described in terms of the running averages $A_j(k)$ to approximate the original time sequence, and running difference $D_j(k)$ to characterize the details of $\boldsymbol{\phi}_H$, where $j = 1, 2, \ldots$ denotes the decomposition level and $k = 1, 2, \ldots$ represents the position. $A_j(k)$ and $D_j(k)$ are defined as $A_j(k) = \sqrt{\frac{1}{T}}\sum_{t=1}^{T}\phi(t)V_{j,k}(t)$ and $D_j(k) = \sqrt{\frac{1}{T}}\sum_{t=1}^{T}\phi(t)W_{j,k}(t)$, where $V_{j,k}(t)$ and $W_{j,k}(t)$ are the Haar scaling and characteristic functions, respectively. Thus at level j of decomposition, ϕ_H is expressed as

$$\phi_H(t) = \sqrt{\frac{1}{T}}\sum_k A_j(k)V_{j,k}(t) + \sqrt{\frac{1}{T}}\sum_{j'=j}^{T-1}\sum_{k}^{2^j-1} D_j(k)W_{j,k}(t) \quad (2)$$

$\mathcal{A}_j$'s and $\mathcal{D}_j$'s are then grouped with the method of hierarchical clustering (HC). HC creates a hierarchical decomposition of ϕ_H, as shown in the dendrogram of Fig. 3(a), from which we can obtain the subsets of input data forming different clusters. Each A_j's and D_j's are grouped into two clusters, including healthy and infarct ones. The clustering results are trained to select the optimal A_{j^*} or D_{j^*} that best represents ϕ_H, so that the clustering results regarding A_{j^*} or D_{j^*} provide the reference of healthy and MI signals.

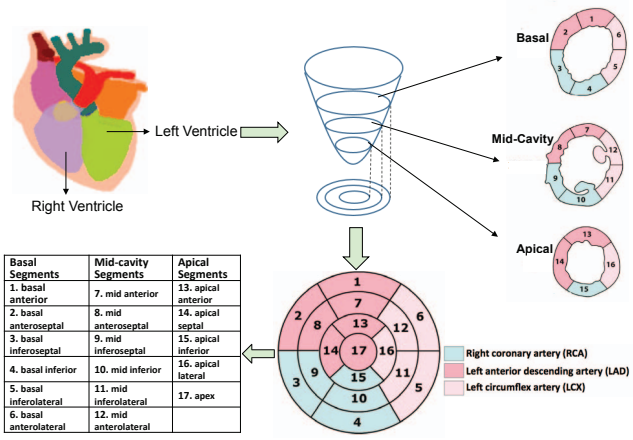

Basal Segments	Mid-cavity Segments	Apical Segments
1. basal anterior	7. mid anterior	13. apical anterior
2. basal anteroseptal	8. mid anteroseptal	14. apical septal
3. basal inferoseptal	9. mid inferoseptal	15. apical inferior
4. basal inferior	10. mid inferior	16. apical lateral
5. basal inferolateral	11. mid inferolateral	17. apex
6. basal anterolateral	12. mid anterolateral	

Fig. 2. 17-segment model of the left ventricle.

D. Performance Metrics

Gadolinium-enhanced transaxial MRI (GE-MRI) provides images for evaluating the proposed ST-iECG model. The extent, centroid and location of MIs are represented by the 17-segment model [6] as shown in Fig. 2.

The proposed ST-iECG model is evaluated with three performance metrics: (1) Percentage discrepancy between the extents of infarction (EPD) as estimated and as given by GE-MRI investigation; (2) Overlap percentage between infarct segments (SO) as estimated and as given by the reference images; (3) Distance from the centroid (CED) of the infarct area as given by GE-MRI images to that as estimated. The three metrics of the proposed ST-iECG model are benchmarked with the results provided by the existing iECG model [1].

III. Experimental Design and Results

A. Wavelet Clustering of ECG Time Series

Four cases including two training cases and two test ones are involved in the experiment. The dataset of BSPMs and the torso-heart geometry is downloaded from the PhysioNet [1] [7]. BSPMs are collected from four patients with one-year MIs, which contain ECG signals for 1000ms at 352 locations on the body surface. And the actual MI segments are shown in GE-MRI images.

The ST-iECG model with λ_s=0.06, $\lambda_t = 0.005$ and $w = 2$ is implemented to solve the iECG problem. The estimated potential distribution ϕ_H is decomposed by Haar

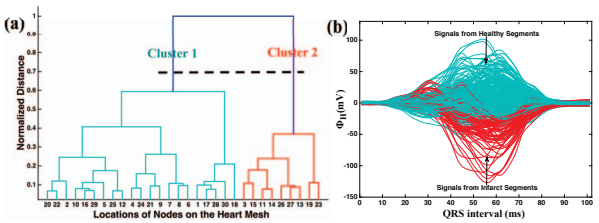

Fig. 3. (a) Hierarchical clustering of case 1. (Note: it just shows the potential signals at a fraction of nodes on the heart mesh because of the space limit.) (b) Clustering results of potential signals in the QRS interval in case 1.

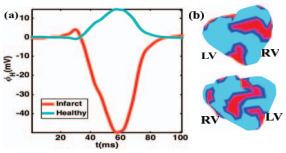

Fig. 4. (a) Averaged potential signals of the healthy and infarct clusters in case 1; (b) Color-coded heart surface with inferior view (top) and anterosuperior view (bottom).

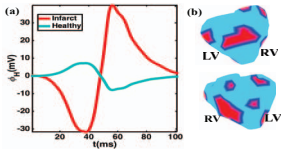

Fig. 5. (a) Averaged potential signals of the healthy and infarct clusters in case 2; (b) Color-coded heart surface with inferior view (top) and anterosuperior view (bottom).

wavelet and characterized with running averages A_j's and running difference D_j's ($j = 1, 2, 3, 4, 5, 6$). Both A_j and D_j are classified into healthy and infarct clusters using HC as shown in Fig. 3(a). A_1 which denotes approximation at level $j = 1$ is selected to represent ϕ_H, by analyzing the clustering results and comparing with reference results given by GE-MRI images. A_1 is then grouped into healthy and MI clusters. Clustering results of the first case regarding the QRS interval in ϕ_H are shown in Fig. 3(b).

B. Experimental Results in Training Case 1 and Case 2

ST-iECG model provides averaged potential signals of the healthy and infarct clusters as shown in Fig. 4(a) and Fig. 5(a). In training case 1, the blue cluster consists of a large portion of positive signals, while signals in red one contain a majority of negative signals. The color-coded heart surfaces derived from these two clusters in case 1 are shown in Fig. 4(b). As shown in Fig. 5(a), the blue cluster consists of fewer negative potentials compared with the red one in case 2. Also, the blue and red areas on the heart surface in Fig. 5(b) represent the corresponding two clusters.

In addition, both color-coded surfaces of case 1 and 2 are projected into 17-segment models in Fig. 6(a) and Fig. 7(a). The true infarct segments in red color provided by GE-MRI images as shown in Fig. 6(b) and Fig. 7(b) for case 1 and case 2, respectively. Comparing segments of two clusters provided by ST-iECG model and GE-MRI images, the red cluster is identified as the MI segments, while the blue one is specified as the healthy cluster.

The extent, infarct segments, and the centroid of MIs in both training cases are summarized in TABLE II. The proposed ST-iECG model yields 29% and 21% of infarct extent in case 1 and 2, respectively. The estimated extents

TABLE II
RESULTS FROM THE PROPOSED ST-IECG INVERSE MODEL, FROM EXITING IECG MODEL [1] AND GE-MRI IMAGES.

Characteristic	Method	Case 1	Case 2	Case 3	Case 4
Extent	GE-MRI	31%	30%	52%	14%
	iECG	25%	35%	35%	40%
	ST-iECG	29%	21%	48%	29%
Infarct Segments	GE-MRI	1,2,3,8,9,13,14,15	3,4,9,10	3,4,5,9,10,11,12,15,16	1,9,10,11,15,17
	iECG	2,3,8,9,14	3,4,5,9,10,11	3,4,5,10,11	3,4,5,6,9,10,11
	ST-iECG	1,2,3,8,9,13,15,16	3,5,9,10	1,3,5,9,10,11,12,16	1,4,5,7,9,15,17
Centroid	GE-MRI	8	3 or 9 or 4 or 10	10 or 11	15
	iECG	9	10	4	4
	ST-iECG	8	10	10 or 11	15

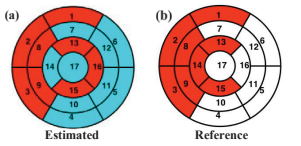

Fig. 6. (a) Estimated MIs (i.e., red segments) by the ST-iECG model of case 1; (b) Reference MIs (i.e., segments colored in red) provided by the GE-MRI image of case 1.

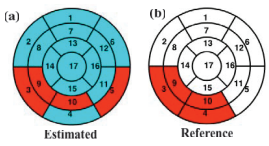

Fig. 7. (a) Estimated MIs (i.e., red segments) by the ST-iECG model of case 2; (b) Reference MIs (i.e., segments colored in red) provided by the GE-MRI image of case 2.

TABLE III
COMPARISON OF PERFORMANCE METRICS IN THE PROPOSED ST-IECG MODEL AND THE EXISTING IECG MODEL [1]

Metric	Method	Case 3	Case 4
EPD	iECG	17%	26%
	ST-iECG	4%	15%
SO	iECG	0.556	0.3
	ST-iECG	0.7	0.444
CED	iECG	1	2
	ST-iECG	0	0

are close to the actual results from GE-MRI images. Infarct segments are estimated accurately except segment 14 in case 1 and segment 4 in case 2. In addition, estimated centroids match real centroids provided by GR-MRI images in both case 1 and case 2.

C. Experimental Results in Test Case 3 and Case 4

As shown in the experimental results in training cases, the cluster with a large portion of negative signals is defined as an infarct cluster, while the one with more positive signals is identified a healthy cluster. The comparison of performance metrics between ST-iECG and iECG [1] of both test cases is summarized in Table III: (1) **EPD**–ST-iECG model contains a lower EPD of 4% in case 3 and 15% in case 4 than iECG model which are 17% and 26% for case 3 and case 4, respectively. This suggests the extent of estimated MIs of the proposed ST-iECG model is closer to actual result as shown in Table II; (2) **SO**–estimation made by ST-iECG overlaps more with actual infarction than iECG, which is indicated by higher SO of ST-iECG compared with iECG shown in Table III; (3) **CED**–distance from the centers given by GE-MRI images to estimated centers by ST-iECG model is zero, while the centers given by iECG are 1 and 2 segments away from the actual centers in test case1 and case 2, respectively.

According to these experimental results of the test cases, the proposed ST-iECG model yields a better performance than the existing iECG model.

IV. CONCLUSIONS

In this paper, we propose a novel ST-iECG model to reconstruct the distribution of electric potentials on the heart surface and further identify the location and extent of MIs. The ST-iECG model is implemented to characterize MIs in four cases and is benchmarked with existing iECG methods. Experimental results show that the cluster with a large portion of positive signals is healthy, while the one with a majority of negative signals is identified as the infarct cluster. In addition, the proposed ST-iECG model achieves a better performance of MI characterization than existing iECG methods. Our ST-iECG model demonstrates a promising potential to characterize the location, extent, and centroid of MIs and provide a valuable support for clinical decision-making in the MI diagnosis and treatment.

REFERENCES

[1] F. Dawoud, G. S. Wagner, G. Moody, and B. M. Horáček, "Using inverse electrocardiography to image myocardial infarctionreflecting on the 2007 physionet/computers in cardiology challenge," *Journal of electrocardiology*, vol. 41, no. 6, pp. 630–635, 2008.

[2] B. Yao, S. Pei, and H. Yang, "Mesh resolution impacts the accuracy of inverse and forward ecg problems," in *Proceedings of 2016 IEEE Engineering in Medicine and Biology Society (EMBC)*, Orlando, FL, 16–20 Aug., 2016, pp. 1–4.

[3] B. Yao and H. Yang, "Physics-driven spatiotemporal regularization for high-dimensional predictive modeling: A novel approach to solve the inverse ecg problem," *Scientific Reports*, vol. 6, p. 39012, 2016.

[4] R. C. Barr, M. Ramsey, and M. S. Spach, "Relating epicardial to body surface potential distributions by means of transfer coefficients based on geometry measurements," *IEEE Transactions on Biomedical Engineering*, no. 1, pp. 1–11, 1977.

[5] P. C. Hansen and D. P. O'Leary, "The use of the l-curve in the regularization of discrete ill-posed problems," *SIAM Journal on Scientific Computing*, vol. 14, no. 6, pp. 1487–1503, 1993.

[6] M. D. Cerqueira, N. J. Weissman, V. Dilsizian, A. K. Jacobs, S. Kaul, W. K. Laskey, D. J. Pennell, J. A. Rumberger, T. Ryan, M. S. Verani *et al.*, "Standardized myocardial segmentation and nomenclature for tomographic imaging of the heart a statement for healthcare professionals from the cardiac imaging committee of the council on clinical cardiology of the american heart association," *Circulation*, vol. 105, no. 4, pp. 539–542, 2002.

[7] A. L. Goldberger, L. A. N. Amaral, L. Glass, J. M. Hausdorff, P. C. Ivanov, R. G. Mark, J. E. Mietus, G. B. Moody, C.-K. Peng, and H. E. Stanley, "PhysioBank, PhysioToolkit, and PhysioNet: Components of a new research resource for complex physiologic signals," *Circulation*, vol. 101, no. 23, pp. e215–e220, 2000.